

Mn doping promotes deep surface reconstruction of CoP nanosheet arrays to drive efficient water splitting

Xiaoyan Liu^a, Tingting Huang^a, Hui Ding^a, Juan Xiao^a, Xiaolan Fan^a, Zhiwei Yu^a, Li Zhang^{*a,b}, Guancheng Xu^{*a}

^a State Key Laboratory of Chemistry and Utilization of Carbon Based Energy Resources, College of Chemistry, Xinjiang University, Urumqi 830017, Xinjiang, PR China

^b College of Chemical Engineering, Xinjiang University, Urumqi 830017, Xinjiang, PR China

Corresponding author

E-mail address: xuguancheng@xju.edu.cn (Guancheng Xu), zhangli420@xju.edu.cn (Li Zhang)

Experimental

1. Chemicals

All chemical reagents were utilized without purification. Coal powder (Heishan, Xinjiang, China) was used as the precursor. Sulfuric acid (H₂SO₄, 95-98%, Xilong Scientific Co., Ltd.), Nitric acid (HNO₃, 65-68%, Xilong Scientific Co., Ltd.), N, N-dimethylformamide (DMF, AR, 99%, Tianjin Zhiyuan Chemical Reagent Co., Ltd.), Polyacrylonitrile (PAN, average Mw=150, 000, Innochem Technology Co., Ltd.), Cobalt chloride hexahydrate (CoCl₂·6H₂O, AR, 99%, Tianjin Xinbote Chemical Co., Ltd.), Manganese(II) Nitrate Tetrahydrate (Mn(NO₃)₂·4H₂O, AR, 98%, Adamas), Potassium hydroxide (KOH, AR, 85%, Tianjin Zhiyuan Chemical Reagent Co., Ltd.), Sodium hypophosphite (NaH₂PO₂·H₂O, AR, 99%, Tianjin Zhiyuan Chemical Reagent Co., Ltd.), commercial Pt/C (20 wt%, JM, Shanghai Hesens Electric Co., Ltd.) and RuO₂ (Shanghai Hesens Electric Co., Ltd.).

2. Materials Characterization

The morphology and detailed microstructures of the final products were characterized by scanning electron microscopy (SEM) with Hitachi S-4800 scanning electron microscope and transmission electron microscopy (TEM) with FEI F30 transmission electron microscope. X-ray diffraction (XRD) patterns were recorded on a Bruker D8 advance X-ray diffractometer with Cu K α radiation source ($\lambda = 1.54178 \text{ \AA}$). Raman spectroscopy was performed on a Bruker Senterra microscope-confocal Raman spectrometer at the excitation wavelength of 532 nm. X-ray photoelectron spectroscopy (XPS) was performed using Thermo Fisher Scientific Escalab 250 Xi with monochromatic Al K α at 15 kW. Element analysis was performed by inductively coupled plasma-mass spectrometry (ICP-MS) using Agilent 7900.

3. Electrochemical Measurements

Accurately cut 0.5 cm × 1 cm of material to be directly used as self-supporting electrode for testing. The Pt/C and RuO₂ electrodes were prepared as follows: accurately weighed the same loading amount of Pt/C and RuO₂ as the final product, and then dispersed them in a mixture of ethanol and deionised water for sonication, and then dropped the Pt/C and RuO₂ onto the 0.5 cm × 1 cm coal-based carbon nanofibers to produce the Pt/C and RuO₂ electrodes, respectively. fibers to produce Pt/C and RuO₂ electrodes.

In this paper, a standard three-electrode test system was used for testing, where the prepared self-supporting electrode was used as the working electrode, the Hg/HgO electrode was used as the reference electrode, and the graphite rod was used as the counter electrode. The electrochemical data were tested on an electrochemical workstation (CHI 660E). The tests of HER performance and OER performance were carried out in 1.0 M KOH electrolyte. A sweep rate of 5 mV s⁻¹ was used for the polarisation curves of the samples in this thesis. All test results were corrected according to the reversible hydrogen electrode (RHE), $E(\text{RHE}) = E(\text{Hg/HgO}) + (0.098 + 0.059 \text{ pH}) \text{ V}$ (1.0 M KOH, pH=14). The voltage interval for the HER performance test was -0.9--1.6 V, the voltage interval for the OER performance test was 0-1.2 V, and the voltage interval for the test of water electrolysis performance was 1.2-2 V. Meanwhile, in order to accurately obtain the overpotentials of the electrocatalysts, the polarisation curves of the HER and the OER in this paper were subjected to 90% iR correction.

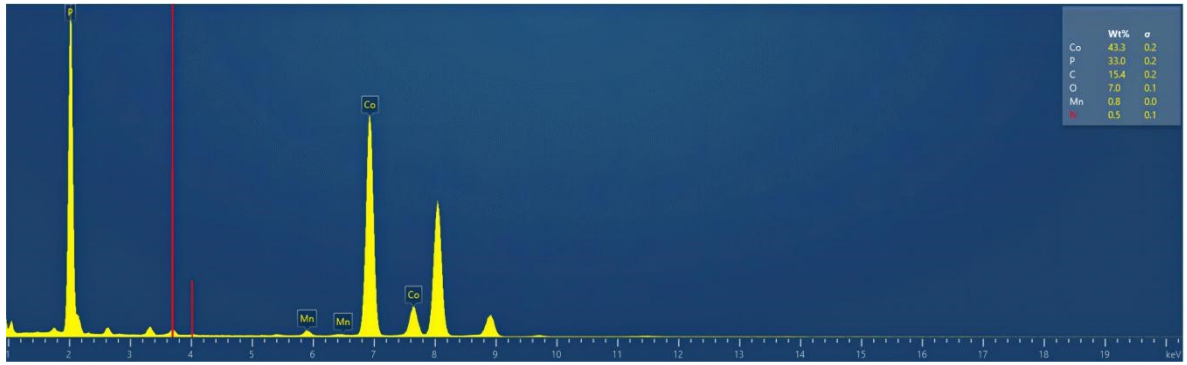


Fig S1. EDX image of Mn₁₀-CoP@C-CNFs.

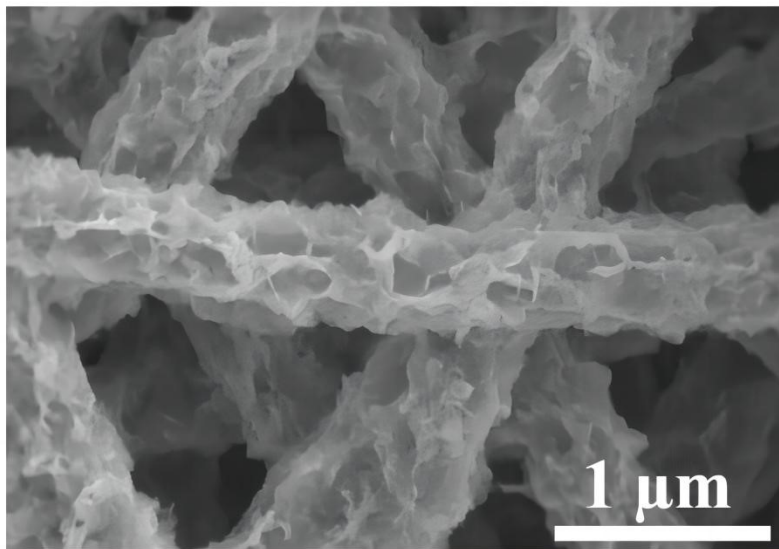


Fig S2. SEM image of the Mn₁₀-CoP@C-CNFs after stability test of HER.

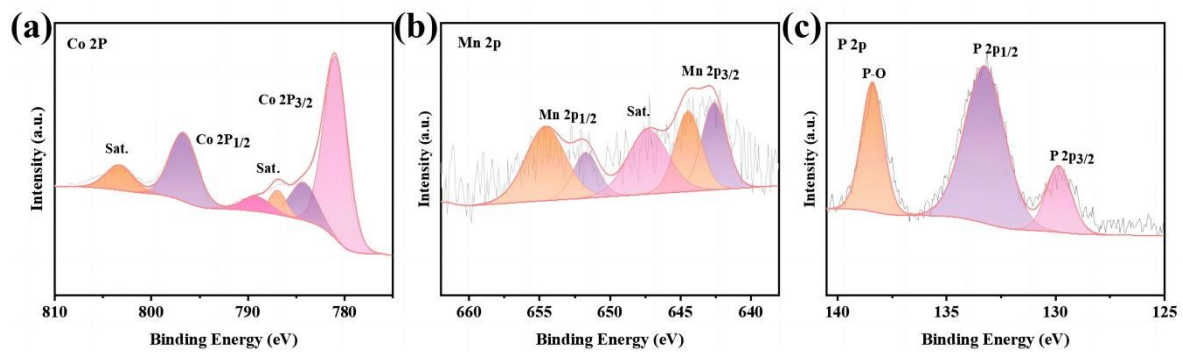


Fig S3. High-resolution XPS spectra of (a) Mn 2p, (b) Co 2p, and (c) P 2p of the Mn₁₀-CoP@C-CNFs after HER stability tests.

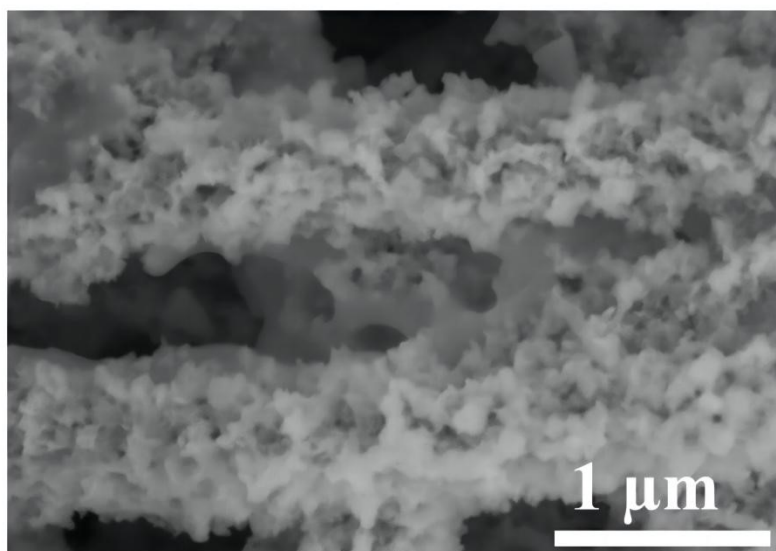


Fig S4. SEM image of the Mn₁₀-CoP@C-CNFs after stability test of OER.

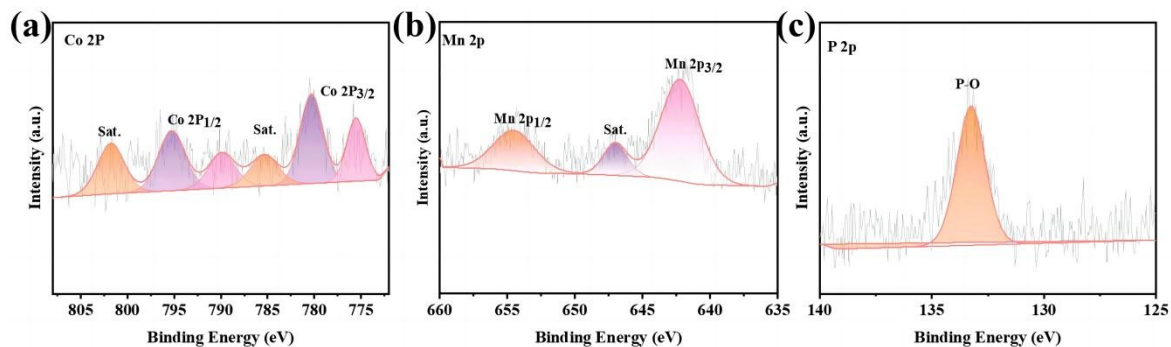


Fig S5. High-resolution XPS spectra of (a) Mn 2p, (b) Co 2p, and (c) P 2p of the Mn₁₀-CoP@C-CNFs after OER stability tests.

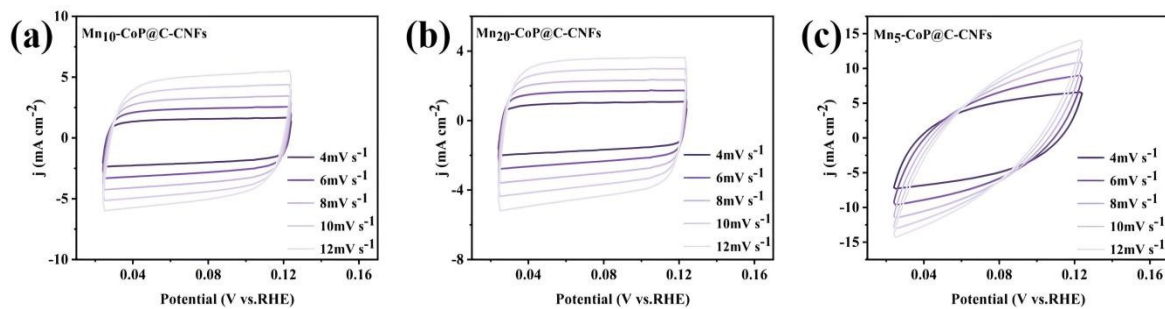


Fig S6. CV scans of (a) Mn₁₀-CoP@C-CNFs, (b) Mn₂₀-CoP@C-CNFs, (c) Mn₅-CoP@C-CNFs at various scan rate for HER.

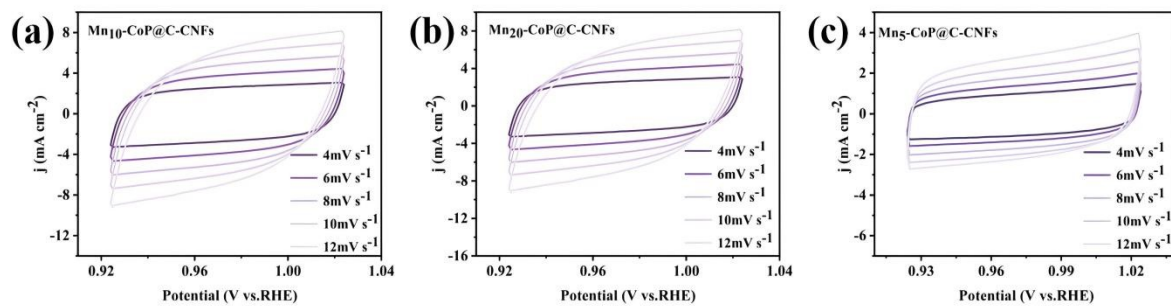


Fig S7. CV scans of (a) $\text{Mn}_{10}\text{-CoP@C-CNFs}$, (b) $\text{Mn}_{20}\text{-CoP@C-CNFs}$, (c) $\text{Mn}_5\text{-CoP@C-CNFs}$ at various scan rate for OER.

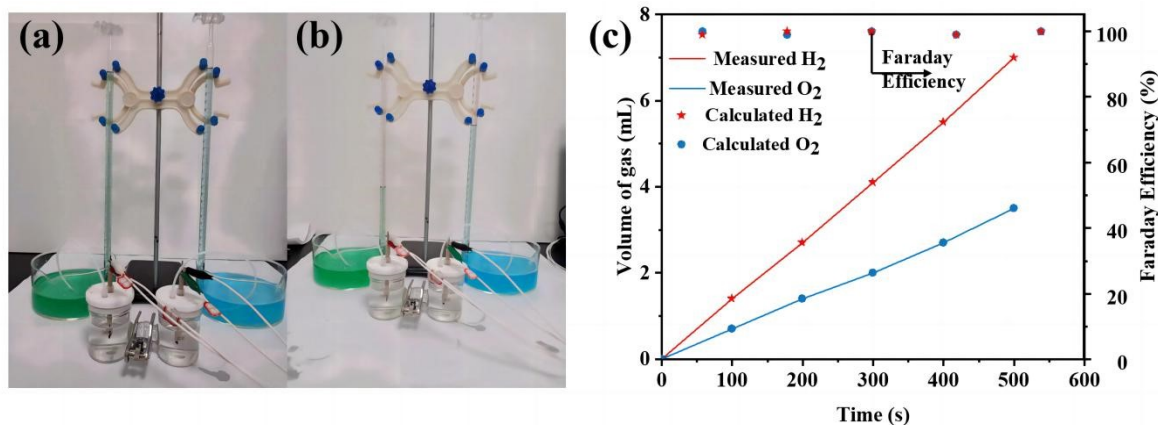


Fig S8. (a, b) Photograph of volume changes during electrocatalytic water splitting, (c) Experimental and theoretical volumes of H_2 and O_2 gases at a current density of 10 mA cm^{-2} and Faraday efficiency of the $\text{Mn}_{10}\text{-CoP@C-CNFs}$.

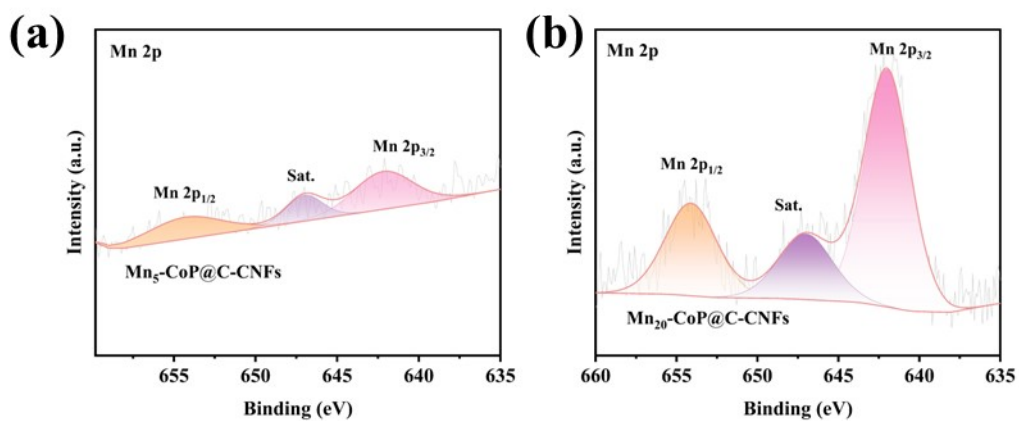


Fig S9. High-resolution XPS spectra of Mn 2p of the (a) Mn₅-CoP@C-CNFs and Mn₂₀-CoP@C-CNFs.

Table S1. Comparison of HER and OER properties of Mn₁₀-CoP@C-CNFs with those of reported representative electrocatalysts under alkaline conditions.

Catalysts	HER	OER	Reference
Mn₁₀-CoP@C-CNFs	62	230	This Work
MnCoP/CC	65	261	1
Mn-CoP/CC	90	/	2
Mn-doped CoP/NF	60	/	3
Mn-Co-P/Ti	76	/	4
Mn-CoP/Co ₂ P	82	309	5
Mn-Ni ₂ P/NF	205	330	6

Table S2. Actual mass ratio of elements in catalysts were acquired by ICP-OES.

Catalyst	Mn/Co
Mn ₅ -CoP@C-CNFs	1: 64.5
Mn ₁₀ -CoP@C-CNFs	1: 55.7
Mn ₂₀ -CoP@C-CNFs	1: 45.9

Reference:

1. M. Wang, W. Fu, L. Du, Y. Wei, P. Rao, L. Wei, X. Zhao, Y. Wang and S. Sun, Surface engineering by doping manganese into cobalt phosphide towards highly efficient bifunctional HER and OER electrocatalysis, *Applied Surface Science*, 2020, **515**.
2. S. Xu, X. Yu, X. Liu, C. Teng, Y. Du and Q. Wu, Contrallable synthesis of peony-like porous Mn-CoP nanorod electrocatalyst for highly efficient hydrogen evolution in acid and alkaline, *Journal of Colloid and Interface Science*, 2020, **577**, 379-387.
3. C. Meng, Z. Wang, L. Zhang, X. Ji, X. Chen and R. Yu, Tuning the Mn Dopant To Boost the Hydrogen Evolution Performance of CoP Nanowire Arrays, *Inorganic Chemistry*, 2022, **61**, 9832-9839.
4. T. Liu, X. Ma, D. Liu, S. Hao, G. Du, Y. Ma, A. M. Asiri, X. Sun and L. Chen, Mn Doping of CoP Nanosheets Array: An Efficient Electrocatalyst for Hydrogen Evolution Reaction with Enhanced Activity at All pH Values, *ACS Catalysis*, 2017, **7**, 98-102.
5. F. Tang, Y.-W. Zhao, Y. Ge, Y.-G. Sun, Y. Zhang, X.-L. Yang, A.-M. Cao, J.-H. Qiu and X.-J. Lin, Synergistic effect of Mn doping and hollow structure boosting Mn-CoP/Co₂P nanotubes as efficient bifunctional electrocatalyst for overall water splitting, *Journal of Colloid and Interface Science*, 2022, **628**, 524-533.
6. P. Xu, L. Qiu, L. Wei, Y. Liu, D. Yuan, Y. Wang and P. Tsiakaras, Efficient overall water splitting over Mn doped Ni₂P microflowers grown on nickel foam, *Catalysis Today*, 2020, **355**, 815-821.